Validation Of A Dynamic PET Simulator In Clinical Brain Studies

Yilong Ma*+, Olivier Rousset*, Peter Neelin*, Alan Evans*, Vijay Dhawan+, David Eidelberg+

*McConnell Brain Imaging Center

Montreal Neurological Institute

McGill University, Montreal, Canada

+Department of Neurology

North Shore University Hospital

New York University School of Medicine, New York, NY 10003

Running title: Validation of a dynamic PET simulator

Correspondence to:

Yilong Ma

Neurology/PET Center

North Shore University Hospital

350 Community Drive

Manhasset, NY 11030

Tel: (516) 562-2498

Fax: (516) 562-1008

Email: yma@nshs.edu

Abstract

This work has been undertaken to evaluate the accuracy of 3-D dynamic simulations in neurological imaging protocols with positron emission tomography (PET). We used [^{18}F]fluorodopa PET images from a pair of normal brain and Parkinsonian brain. Spatially correlated MR images were segmented into several tissue types and anatomical structures. Voxels within every structure were assigned with the time activity curves (TACs) derived from clinical studies after correcting for partial volume effects. Both noisefree and noisy projection data of this brain model were created and reconstructed as in the real scans. TACs were then generated from the dynamic images and compared with the measured data. The results show good agreement between the simulated and observed TACs in the normal brain. However the match is poorer in the Parkinson's brain particularly in striatal structures. This suggests a possible mismatch between the simulated true activity distribution and that in the diseased brain. Both normal and patient data have root-mean-square errors of 2% in cortical gray matter and <10% in striatum without and with noise. This tool can be used to optimize temporal sampling strategy and parameter estimation algorithms.

1 Introduction

Positron emission tomography (PET) permits quantitative analysis of a wide array of biological markers in the living human brain. This has become an important methodology to probe metabolic and pharmacokinetic processes in both healthy brains and neurological diseases. However clinical images are heavily smoothed to suppress statistical noise, resulting in relatively poor image resolution and nonlinear partial volume distortions in many functional brain structures.

Estimation of physiological parameters with PET poses serious problems because of unknown bias and variance in recorded time-activity curves (TACs). The problems are normally evaluated by performing simple simulations on a set of tissue TACs which ignore object and camera dependent distortions [1, 2]. While this method is useful for relative comparisons of tracer kinetic models it generally gives very limited information. Any practical solution to this type of problems must consider contributions from data acquisition and reconstruction algorithms specific to each PET imaging experiment.

Simulation tools based on projection data have been used in several imaging centers to compare image processing or restoration algorithms [8, 4]. By modeling image acquisition from raw data this approach allows correct simulation of the magnitude and distribution of noise in the image space. However none of the previous methods have been validated. We have implemented a comprehensive PET simulator by combining tomograph physical characteristics with realistic tracer biodistribution data and segmented MR images. It models 3-D resolution, attenuation, scatter, randoms and Poisson statistics as described previously [6]. This chapter describes a preliminary study to validate its performance in clinical brain scans. We want to demonstrate the usage of computer simulations in both normal brain function and pathological cases.

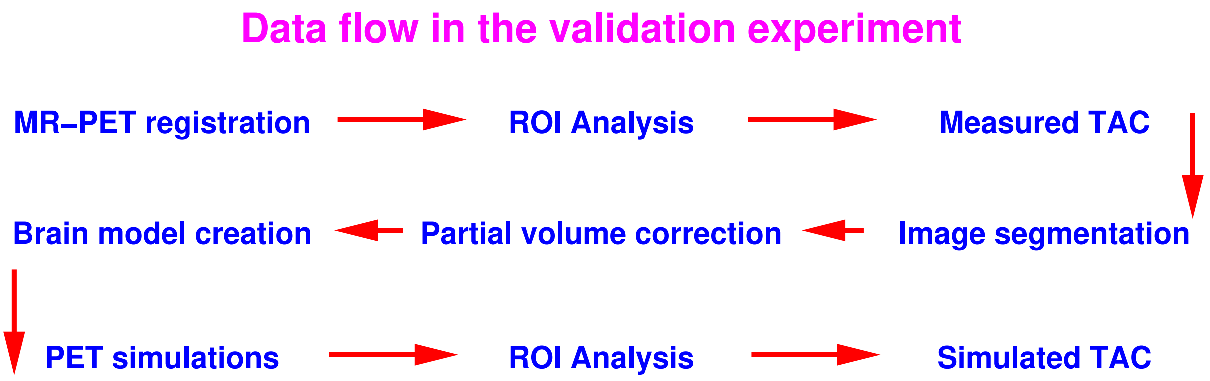

Figure 1: A block diagram showing the generation of simulated time activity curves from the measured data.

2 Materials and Methods

The chief goal of this work is to generate simulated regional TACs and compare the results with the clinical measurements from the scanner. This is based on several experimental procedures illustrated schematically in Fig. 1 and computation steps are summarized below.

2.1 Clinical Image Data

We used typical MR data and PET images of F-Dopa acquired from a normal subject and a patient with Parkinson's disease. Each subject had MRI scan as part of the PET imaging protocol. This was done on a Philips 1.5 T scanner employing a 3-D gradient echo sequence (TE = 10.3 ms, TR = 18 ms, Flip angle = 30°, NEX = 1). Images were saved as 128 256 x 256 slices with a voxel size of 1 x 1 x 1 mm^3.

PET images were obtained on a Scanditronix PC2048 brain scanner following a bolus injection of 5 mCi F-Dopa. The total scan duration was 90 min with a time sequence of 6 x 0.5 min, 7 x 1 min, 5 x 2 min, 4 x 5 min, 5 x 10 min. Image volumes consisted of 27 frames and were reconstructed with a 12 mm Hanning filter. Images were stored on a 15 x 128 x 128 matrix with a voxel size of 6 x 2 x 2 mm^3.

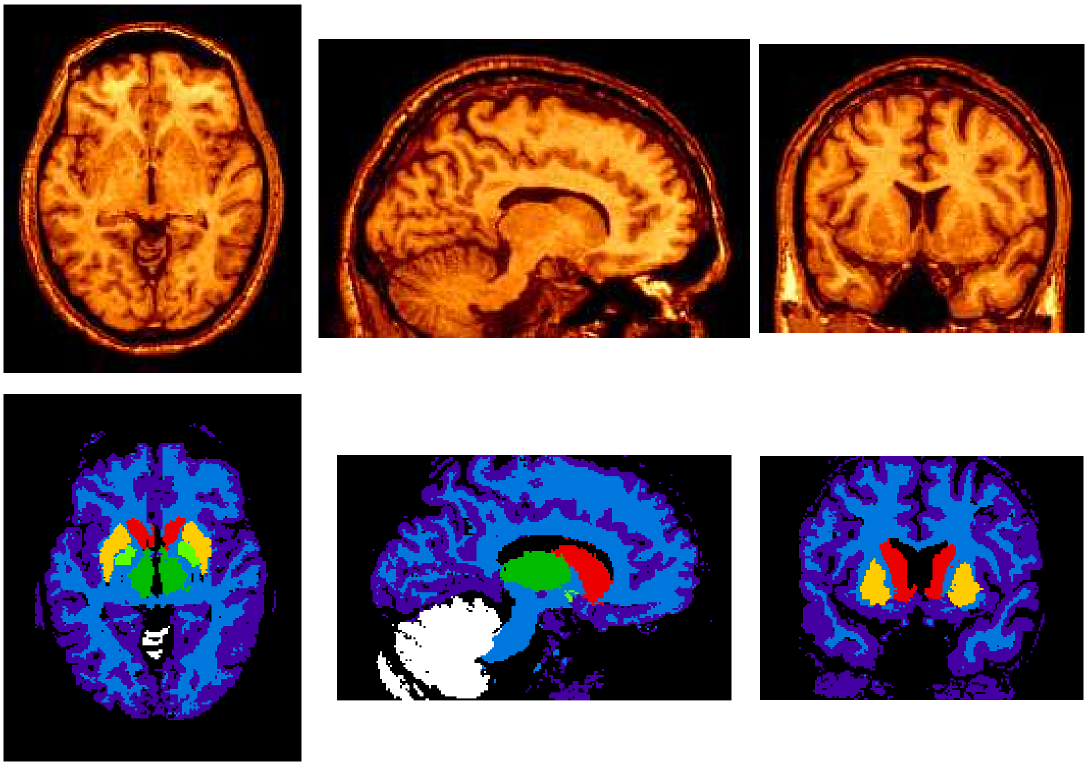

Figure 2: Volumetric MR images and segmented tissue maps in the 3-D brain phantom. Note the clear delineation of striatum, thalamus and cerebellum. Both imaging volumes are created after registration with the PET data.

2.2 Individual Brain Model

In each case MRI data were spatially registered to PET transmission images automatically. This method provided better MR-PET registration in neuroreceptor PET imaging studies as compared with conventional approaches based on emission images. TACs were then extracted in gray matter (GM), white matter (WM), caudate nucleus (CN) and putamen (PU) using regional masks drawn from MRI data. A 3-D brain phantom was created by segmenting the MRI volume into a set of functional and anatomical structures. Tissue maps and small structures were labeled using an automated tissue classifier and semiautomatic tools respectively. Fig. 2 shows typical MR images and distinct tissue types used in this study.

In order to obtain true regional values of F-Dopa uptake we performed a fully 3-D partial volume correction to the observed TACs [7]. The accuracy of this method has been validated using a 3-D brain phantom of human basal ganglia. To remove local variability and statistical uncertainty inherent in the corrected data we computed an average

$$A_i = \sum_{j}^{N} T_j a_j \tag{1}$$

where T_j and a_j are the corrected TAC and geometric area of each ROI and N the total number of ROIs over several slices and both hemispheres. In order to further reduce potential errors from discrete time sampling, the resulting values A_i were fitted by linear regression (Fig. 3).

In this preliminary analysis we assume that the tracer is uniformly distributed over the volume of each tissue. Thus we assigned the corrected TAC to each tissue in the segmented brain phantom to represent true activity distribution of Fdopa accumulation. Soft tissue and skull bone were also assigned with appropriate photon attenuation values.

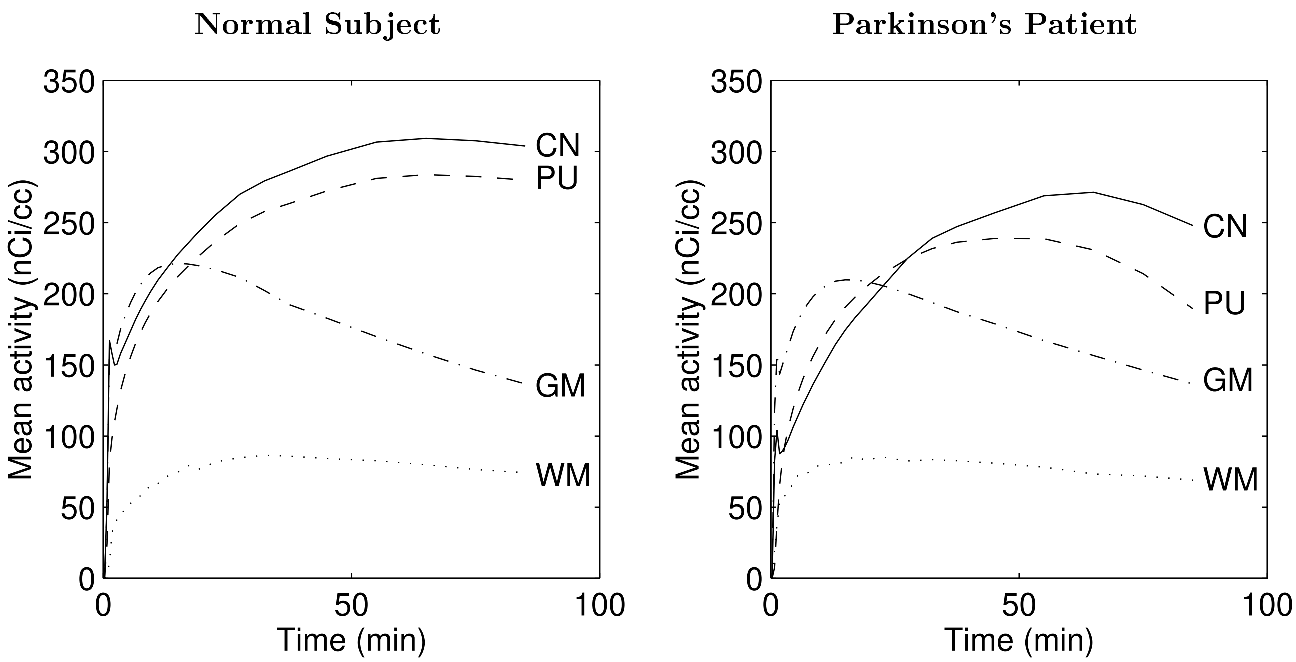

Figure 3: True tissue time-activity curves in gray matter (GM), white matter (WM), caudate nucleus (CN) and putamen (PU).

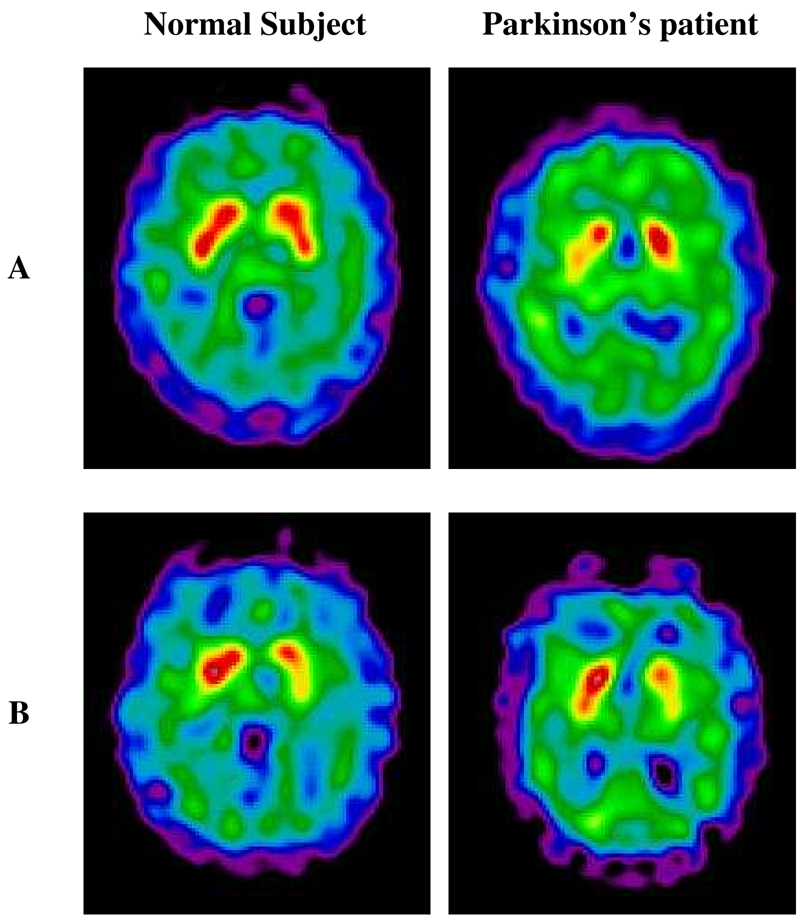

Figure 4: Real (A) and simulated (B) F-dopa images with the highest tracer uptake in the striatum. Images contain about 300 K slice counts and reconstructed with a 12 mm Hanning filter.

2.3 Dynamic Simulations

A series of projection data were simulated with all the physical effects in PET scans as described elsewhere [6]. This included photon attenuation and scatter modeling in addition to other camera and study specific factors. The resulting data were reconstructed into tomographic images using the scanner reconstruction program. Both procedures were done using acquisition and reconstruction parameters that were identical to the real scan data. TACs were then generated from the dynamic images with and without counting noise. Comparison with the measured real data was performed

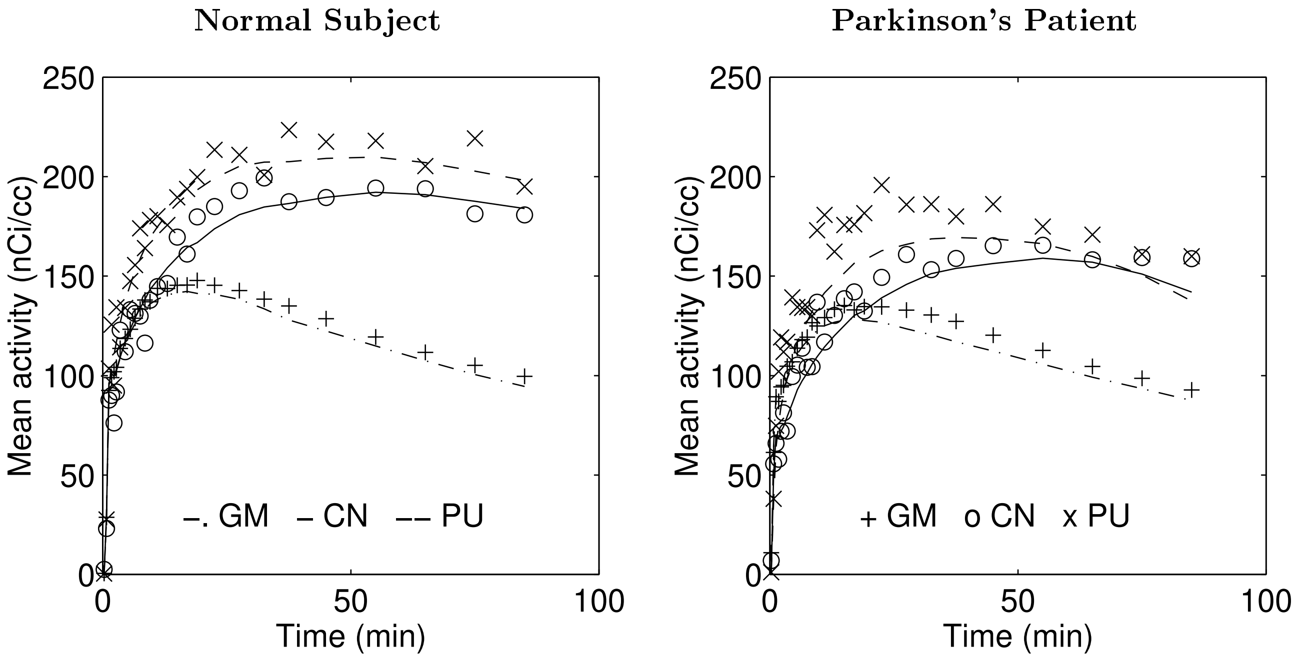

Figure 5: Simulated (lines) and real (symbols) time-activity curves in gray matter (GM) and striatal structures (CN, PU). Data are mean values over basal ganglia slices on both sides of the brain.

by computing the root-mean-square (rms) distances of the relative discrepancy

$$D_i = \frac{(A_s - A_r)}{A_r} \tag{2}$$

averaged over frames. A_s and A_r represented the TACs from the simulated and scan data respectively. The first time point was excluded from the calculation since it approaches zero.

3 Results and Discussion

Simulation results reproduce general patterns of F-Dopa PET images in both subjects (Fig. 4). Fig. 5 presents TACs in gray matter, caudate nucleus and putamen. It shows good agreement between the simulated and observed TACs in the normal brain. We see similar results after adding Poisson noise in the projection data. This implies that anatomical structures and activity concentrations in the 3-D brain model correlate with the uptake regions of F-Dopa in the normal brain.

Table 1: Percentage root-mean-square distances between regional data

Noise	GM	WM	CN	PU
	Normal Subject			
No	1.31	2.73	8.28	4.51
Yes	1.37	2.40	8.70	8.63
	Parkinson's Patient			
No	2.11	2.24	5.41	7.14
Yes	2.05	2.52	5.61	6.51

Values are calculated from (simulation - real)/real averaged over the dynamic frames. Notice the similarity between the noiseless and noisy data.

However we observe a somewhat poor match in the Parkinson's brain, particularly in the basal ganglia (Fig. 5). This may come from several sources. The first one is inhomogeneity of radioactivity distribution in the diseased brain. Secondly striatal structures derived from MR images may not correspond to uptake areas of F-Dopa visualized on PET scans. Table 1 lists the rms distances. Both normal and patient data have rms errors of 2% in gray matter, 3% in white matter and <10% in striatum without and with noise. The residual discrepancy is likely to stem from small PET-MRI misregistration and possible errors in MR image segmentation.

The large differences between the observed and true TACs reflect partial volume problems as we have documented before. Note that the true kinetic curves in Fig. 3 show higher caudate uptake in both normal and Parkinson's diseases about 20 minutes after the injection. However the observed TACs in caudate are lower than those in putamen. This is expected since caudate is generally smaller than putamen across the brain volume and the data are averaged over basal ganglia slices and left-right sides of the brain. More importantly the data shown here demonstrate that partial volume effects can drastically alter the kinetic relationship between normal and Parkinson's brain. It suggests that the use of uncorrected data may impair accurate diagnosis of disease severity.

A much simpler simulation is widely used to compare kinetic data analysis algorithms. It usually works by solving compartmental equations while adding varying amount random noise to theoretical TACs [1, 2]. This type of work has limited value since it ignores image bias and variance introduced by the projection and backprojection process. To avoid such problems several groups have developed projection-based simulation tools for PET brain images. We have expanded the previous methods and validated the simulated data and images with brain phantoms [6]. In particular the technique allows us to simulate both emission and transmission scans rapidly.

The work reported here represents the first attempt to compare simulations with clinical data. This could not be achieved in the past because the measured data are always biased by partial volume effects. By correcting the bias explicitly we have now overcome this obstacle. Since the true activity distribution in the brain is known this permits more realistic evaluation of many neuroimaging methods operating at both pixel and regional levels. One useful example is the automatic tissue segmentation algorithms based on unique features of TACs in different cerebral structures [3]. Recently there has been growing interest to probe ligand and receptor interactions with multiple radiotracers. Simulations using a Hoffman brain phantom have demonstrated the feasibility of performing a dual-tracer paradigm in a single session [5]. The methods validated here rely on both structural and functional data of the individual brain. With proper use, this powerful tool offers an objective basis to design optimal imaging protocols in a large number of clinical applications.

4 Summary

In this chapter we have simulated and compared dynamic data from F-dopa PET imaging in the human brain. Preliminary data indicate that the simulated and measured TACs match with reasonably good accuracy. It is still necessary to model spatially variant tracer distribution from MR images and clinical uptake information. Nevertheless the results presented here confirm the validity of the PET simulator in predicting the shape and magnitude of TACs in normal and abnormal brains. This would allow researchers to evaluate data acquisition and analysis methods in clinical imaging studies. One immediate use is to optimize temporal sampling strategy and parameter estimation algorithms.

References

[1] G. Blomqvist, A.A. Lammertsma, B. Mazoyer, and K. Wienhard. Effect of tissue heterogeneity on quantification in positron emission tomography. *Eur. J. Nucl. Med.*, 22:652–663, 1995.

[2] D. Feng, K.P. Wong, C.M. Wu, and W.C. Siu. Simultaneous extraction of physiological and input function parameters from PET measurements. In R.E. Carson, M.E. Daube-Witherspoon, and P. Herscovitch, editors, *Quantification of brain function using PET*, pages 321–327, San Diego, 1998. Academic Press.

[3] R.N. Gunn, A. Lammertsma, and V. Cunningham. Parametric imaging of ligand-receptor interactions using a reference tissue model and cluster analysis. In R.E. Carson, M.E. Daube-Witherspoon, and P. Herscovitch, editors, *Quantification of brain function using PET*, pages 401–406, San Diego, 1998. Academic Press.

[4] S.C. Huang, J. Yang, C.L. Yu, and K.P. Lin. Performance characteristics of a feature-matching axial smoothing method for brain PET images. In R.E. Carson, M.E. Daube-Witherspoon, and P. Herscovitch, editors, *Quantification of brain function using PET*, pages 85–90, San Diego, 1998. Academic Press.

[5] R.A. Koeppe, E.P. Ficaro, D.M. Raffel, S. Minoshima, and M.R. Kilbourn. Temporally overlapping dual tracer PET studies. In R.E. Carson, M.E. Daube-Witherspoon, and P. Herscovitch, editors, *Quantification of brain function using PET*, pages 359–366, San Diego, 1998. Academic Press.

[6] Y. Ma and A.C. Evans. Analytical modeling of PET imaging with correlated functional and structural images. *IEEE Trans. Nucl. Sci.*, 44:2439–2444, 1997.

[7] O. Rousset, Y. Ma, and A.C. Evans. Correction for partial volume effects in PET: principle and validation. *J. Nucl. Med.*, 39(5):904–911, May 1998.

[8] S. Sastry and R.E. Carson. Multimodality Bayesian algorithm for image reconstruction in PET: a tissue composition model. *IEEE Trans. Med. Imag.*, 16:750–761, 1997.

Acknowledgments

This work was supported by the Medical Research Council of Canada and the International Consortium on Brain Mapping. The authors gratefully acknowledge the excellent technical assistance from the staff at the Brain Imaging Center for carrying out MRI and PET studies.